




Forecasting Constraint on the $f(R)$ Theory with the CSST SN Ia and BAO Surveys

Jun-Hui Yan^{1,2}, Yan Gong^{1,2,3}, Minglin Wang^{1,2}, Haitao Miao^{1,2}, and Xuelei Chen^{1,2,4,5} 

¹ National Astronomical Observatories, Chinese Academy of Sciences, Beijing 100101, China; gongyan@bao.ac.cn

² University of Chinese Academy of Sciences, Beijing 100049, China

³ Science Center for China Space Station Telescope, National Astronomical Observatories, Chinese Academy of Sciences, Beijing 100101, China

⁴ Department of Physics, College of Sciences, Northeastern University, Shenyang 110819, China

⁵ Centre for High Energy Physics, Peking University, Beijing 100871, China

Received 2024 July 24; revised 2024 September 19; accepted 2024 October 14; published 2024 November 5

Abstract

The $f(R)$ modified gravity theory can explain the accelerating expansion of the late Universe without introducing dark energy. In this study, we predict the constraint strength on the $f(R)$ theory using the mock data generated from the Chinese Space Station Telescope (CSST) Ultra-Deep Field Type Ia supernova (SN Ia) survey and wide-field slitless spectroscopic baryon acoustic oscillation (BAO) survey. We explore three popular $f(R)$ models and introduce a parameter b to characterize the deviation of the $f(R)$ theory from the Λ CDM theory. The Markov Chain Monte Carlo method is employed to constrain the parameters in the $f(R)$ models, and the nuisance parameters and systematic uncertainties are also considered in the model fitting process. Besides, we also perform model comparisons between the $f(R)$ models and the Λ CDM model. We find that the constraint accuracy using the CSST SN Ia+BAO data set alone is comparable to or even better than the result given by the combination of the current relevant observations, and the CSST SN Ia+BAO survey can distinguish the $f(R)$ models from the Λ CDM model. This indicates that the CSST SN Ia and BAO surveys can effectively constrain and test the $f(R)$ theory.

Key words: (cosmology:) cosmological parameters – cosmology: theory – (cosmology:) dark energy

1. Introduction

The late-time acceleration of the Universe, first observed by the High- z Supernova Search Team (Riess et al. 1998) and the Supernova Cosmology Project (Perlmutter et al. 1999), has posed a significant puzzle in modern cosmology. General relativity (GR) is widely accepted as the fundamental theory describing the geometric properties of spacetime, with the Einstein field equations yielding the Friedman equations that describe the evolution of the Universe within the framework of GR. Introducing a new dark energy component in this framework has proven effective in describing standard cosmology based on radiation and matter-dominated epochs, corresponding to the conventional Big Bang model.

Theoretical efforts to account for this phenomenon within the confines of GR face challenges, prompting the need for novel explanations or modifications to the existing framework. The modified gravity theory of $f(R)$, which has gained widespread attention, presents a theoretical framework for gravitational corrections. The $f(R)$ modified gravity theory introduces a novel perspective wherein the curvature scalar R is allowed to take on any arbitrary function $f(R)$ rather than being linear. By incorporating this additional degree of freedom, the $f(R)$ theory can address phenomena that are not adequately explained by GR (Saridakis et al. 2021), thereby providing a new theoretical framework for cosmology and cosmic evolution.

As early as the 1980s, a modified gravity model was proposed by Starobinsky to explain inflation (Starobinsky 1980). Subsequently, with the discovery of cosmic acceleration during the late stages of the Universe (Riess et al. 1998; Perlmutter et al. 1999), the $f(R)$ theory began to be considered as a tool for explaining this phenomenon. Basilakos et al. (2013) introduced a method for solving ordinary differential equations (ODEs) using series expansions to obtain the Hubble parameter, enabling a more efficient constraint of the $f(R)$ theory using cosmological observations. In terms of kinematics, Kumar et al. (2023) utilized the latest Type Ia supernova (SN Ia) data and conducted a joint analysis with baryon acoustic oscillations (BAOs) and Big Bang nucleosynthesis (BBN) to provide updated observational constraints on two $f(R)$ gravity models (Hu–Sawicki and Starobinsky models). They found slight evidence for $f(R)$ gravity under the dynamics of Hu–Sawicki, but the inclusion of progenitor distances made the model compatible with GR. Dainotti et al. (2024) performed a binning analysis of PantheonPlusSH0ES, obtaining different values of H_0 , and proposed that H_0 undergoes a slow decline with z , speculating that the $f(R)$ modified gravity theory is an effective model for explaining this trend. Qi et al. (2023) studied the late-time dynamics of the Universe under the $f(R)$ model and obtained feasible late-time cosmological models through parameter tuning. They compared these models with the Λ CDM model

using SN Ia data and found good agreement between theory and data.

Undoubtedly, future SN Ia and BAO observations will provide more stringent constraint on the $f(R)$ theory, such as the Legacy Survey of Space and Time (LSST Dark Energy Science Collaboration 2012), Euclid (Casas et al. 2023), Dark Energy Spectroscopic Instrument (Casas et al. 2023), etc. The Chinese Space Station Telescope (CSST) is a next-generation Stage IV 2 m sky survey telescope. It is designed for simultaneous photometric imaging and slitless grating spectroscopic measurements. Over approximately 10 yr of observation, the CSST will cover a sky area of $17,500 \text{ deg}^2$, with a field of view of 1.1 deg^2 . Its wavelength coverage ranges from near-ultraviolet to near-infrared, with seven photometric and three spectroscopic bands. Besides, the CSST also can perform a 9 deg^2 Ultra-Deep Field (UDF) survey for observing high- z galaxies and SNe Ia (Wang et al. 2024). Therefore, through the observations of weak gravitational lensing, galaxy clustering, SNe Ia, and other cosmological probes, the CSST can reconstruct the history of cosmic expansion and structure growth with high-precision, and hence provide accurate constraints on the modified gravity models, enabling a rigorous distinction between dark energy and modified gravity theories on cosmological scales.

In this study, we predict the constraint on different $f(R)$ theories using the mock data of the CSST SN Ia (Wang et al. 2024) and BAO (Miao et al. 2023) observations. All the simulations were obtained based on the flat Universe of Planck Collaboration et al. (2020), and the fiducial values of our cosmological parameters were set to $[h, \Omega_{m0}, \Omega_{b0}, b, A_s, n_s, N_{\text{eff}}] = [0.673, 0.313, 0.0049, 0, 2.099 \times 10^{-9}, 0.965, 3.04]$, where b is a parameter introduced by the modification of the gravitational theory by $f(R)$. Our approach involves a comprehensive analysis that integrates these observational data sets to refine and narrow down the permissible parameter space within the context of the modified gravity theory $f(R)$. The structure of this paper is as follows: we introduce the basic cosmological theory related to the $f(R)$ theory and the method of obtaining the Hubble parameters under $f(R)$ models in Section 2; in Section 3 we discuss the relevant mock data we use; in Section 4 we show the parameter constraint and the model comparison methods used in this work. We give the results and summary in Sections 5 and 6 respectively.

2. Cosmology of $f(R)$ Theory

2.1. $f(R)$ Basics

By modifying the Einstein–Hilbert action of GR, the $f(R)$ theory can be derived by (Nojiri & Odintsov 2011; Nojiri et al. 2017)

$$S = \int d^4x \sqrt{-g} \left(\frac{f(R)}{16\pi G} + \mathcal{L}_m + \mathcal{L}_r \right). \quad (1)$$

Here $f(R)$ denotes the function of Ricci scalar R , and \mathcal{L}_m and \mathcal{L}_r represent the Lagrangian densities for matter and radiation,

respectively. The field equations for the $f(R)$ theory are obtained by varying Equation (1), and we have

$$f_R G_{ab} - \frac{1}{2} g_{ab} f + \frac{1}{2} g_{ab} f_R R - \nabla_a \nabla_b f_R + g_{ab} \square f_R = 8\pi G [T_{ab}^{(m)} + T_{ab}^{(r)}], \quad (2)$$

where f is the simple form of $f(R)$, and f_R denotes the first derivative of $f(R)$ with respect to R . We assume that the presence of an ideal fluid in the Universe is composed of cold dark matter and radiation. $T_{ab}^{(m)}$ and $T_{ab}^{(r)}$ represent the energy-momentum tensors for the matter sector and the radiation sector, respectively. For a spatially flat Universe and assuming the Friedmann–Lemaître–Robertson–Walker metric, Equation (2) gives

$$3f_R H^2 = 8\pi G(\rho_m + \rho_r) + \frac{1}{2}(f_R R - f) - 3H\dot{f}_R, \quad (3)$$

$$-2f_R \dot{H} = 8\pi G(\rho_m + p_m + \rho_r + p_r) + \ddot{f}_R - H\dot{f}_R. \quad (4)$$

Here H is the Hubble parameter, and ρ_x and p_x are the energy density and pressure for matter or radiation, respectively. We can define the effective energy density and pressure ρ_{eff} and p_{eff} as (De Felice & Tsujikawa 2010)

$$\rho_{\text{eff}} \equiv \frac{1}{8\pi G} \left(\frac{1}{2}(f_R R - f) - 3H\dot{f}_R + 3(1 - f_R)H^2 \right), \quad (5)$$

$$p_{\text{eff}} \equiv \frac{1}{8\pi G} \left[-\frac{1}{2}(f_R R - f) - (1 - f_R)(2\dot{H} + 3H^2) + \ddot{f}_R + 2H\dot{f}_R \right]. \quad (6)$$

Then we obtain the modified Friedmann's equations in the $f(R)$ theory

$$3f_R H^2 = 8\pi G(\rho_m + \rho_r + \rho_{\text{eff}}) + \ddot{f}_R - H\dot{f}_R, \quad (7)$$

$$2f_R \dot{H} = -8\pi G(\rho_m + \frac{4}{3}\rho_r). \quad (8)$$

The effective equation of state of the $f(R)$ gravity can be written as

$$w_{\text{eff}} \equiv \frac{p_{\text{eff}}}{\rho_{\text{eff}}} = -1 - \frac{H\dot{f}_R + 2\dot{H} - 2f_R \dot{H} - \ddot{f}_R}{\frac{1}{2}(f_R R - f) - 3H\dot{f}_R + 3(1 - f_R)H^2}. \quad (9)$$

We can easily find the deviation of w_{eff} from -1 due to the modified gravitational theory in this form.

The current observations of the Cosmic Microwave Background have validated the reliability of the Λ CDM cosmological model in the high-redshift regime. Consequently, the cosmology under the $f(R)$ theory is expected to closely approximate the Λ CDM cosmology at high redshifts. Simultaneously, the Λ CDM model successfully predicts the phenomenon of late-time cosmic acceleration. Hence, the Universe described by the $f(R)$ theory should also exhibit accelerating expansion at low redshifts without introducing a true cosmological constant. The requirements mentioned above

can be summarized as follows (Hu & Sawicki 2007)

$$\begin{aligned} \lim_{R \rightarrow \infty} f(R) &= R - 2\Lambda, \\ \lim_{R \rightarrow 0} f(R) &= R. \end{aligned} \quad (10)$$

An $f(R)$ model also needs to avoid several problems such as matter instability (Faraoni 2006), the instability of cosmological perturbations (Bean et al. 2007), the absence of the matter (Chiba et al. 2007) era and the inability to satisfy local gravity constraints (Nojiri & Odintsov 2006), thus viable $f(R)$ models must satisfy the following conditions (Starobinsky 2007; Basilakos et al. 2013)

$$f_R > 0 \text{ and } f_{RR} > 0, \text{ for } R \geq R_0(>0), \quad (11)$$

$$0 < \left(\frac{Rf_{RR}}{f_R} \right)_{r=-2} < 1, \quad (12)$$

where f_{RR} denotes the second derivative of $f(R)$ with respect to R , R_0 is the value of R today and $r \equiv -Rf_R/f$. We are reminded that if the final attractor is a de Sitter point, we also need $f_R > 0$ for $R \geq R_1(>0)$, where R_1 is the Ricci scalar at the de Sitter point.

2.2. $f(R)$ Models

The current $f(R)$ models usually can be equivalent to the perturbations of the Λ CDM theory, so their general form can be written in the following parameterized form

$$f(R) = R - 2\Lambda y(R, b), \quad (13)$$

where $\lim_{R \rightarrow \infty} y(R, b) = 1$ and $\lim_{R \rightarrow 0} y(R, b) = 0$ to satisfy the conditions presented in Equation (10).

Hu & Sawicki (2007) proposed an $f(R)$ model that accelerates the cosmic expansion without a cosmological constant, and satisfies both cosmological and solar system tests in the small-field limit of the parameter space, which takes the form of

$$f(R) = R - m^2 \frac{c_1(R/m^2)^n}{c_2(R/m^2)^n + 1}, \quad (14)$$

where $m^2 \equiv \kappa^2 \bar{\rho}_0/3$ relates to $\kappa^2 = 1/16\pi G$, the average density today is $\bar{\rho}_0$, and c_1 and c_2 are dimensionless parameters. In the study by Capozziello & Tsujikawa (2008), it was suggested that n is an integer. Therefore, for simplicity, we consider the case where $n=1$, and then we can rewrite Equation (14) in a parameterized form as Equation (13)

$$f_{\text{HS}}(R) = R - \frac{2\Lambda}{1 + \left(\frac{b\Lambda}{R}\right)^n}, \quad (15)$$

where $\Lambda = m^2 c_1/c_2$, $b = 2c_2^{1-1/n}/c_1$ and $y_{\text{HS}}(R, b) = \left[1 + \left(\frac{b\Lambda}{R}\right)^n\right]^{-1}$. It can be noted that when $b \rightarrow 0$ (or equally $c_1 \rightarrow \infty$), we have $f(R) \rightarrow R - 2\Lambda$, i.e., the Hu–Sawicki model returns to the Λ CDM model.

Moreover, Starobinsky (2007) also proposed an $f(R)$ model, which is given by

$$f_{\text{St}}(R) = R - c_1 m^2 \left[1 - \frac{1}{(1 + R^2/m^4)^n} \right]. \quad (16)$$

Similarly, when $\Lambda = \frac{c_1 m^2}{2}$, $b = \frac{2}{c_1}$ and $y_{\text{St}}(R, b) = 1 - \left(1 + \left(\frac{R}{b\Lambda}\right)^2\right)^{-n}$, Equation (16) can be rewritten as

$$f_{\text{St}}(R) = R - 2\Lambda \left\{ 1 - \left[1 + \left(\frac{R}{b\Lambda}\right)^2 \right]^{-n} \right\}. \quad (17)$$

We can find that the Starobinsky model will return to the Λ CDM model when $b=0$.

In addition, an alternative parameterization is also mentioned in Pérez-Romero & Nesseris (2018), which can be expressed by

$$f(R) = R - \frac{2\Lambda}{1 + bp(R, \Lambda)}. \quad (18)$$

This model under this parameterization method also yields an expansion history similar to the expansion history of Λ CDM, as well as a specific expression for the Hubble parameter via the modified Friedman equation. Here we use a parameterized model of $f(R)$ in which the form $p(R, \Lambda)$ is $\text{ArcTanh}(R, \Lambda)$, i.e.,

$$f_{\text{AcT}}(R) = R - \frac{2\Lambda}{1 + b\text{ArcTanh}(\Lambda/R)}. \quad (19)$$

It can be seen that when $b=0$, the ArcTanh model will also return to the Λ CDM model. We will discuss the constraints on these three $f(R)$ models in the CSST SN Ia and BAO surveys.

Besides, in other studies (e.g., Koyama 2016; Liu et al. 2016), the background strength of modified gravity, f_{R0} , is also employed to characterize the difference between modified gravity and GR, where f_{R0} is defined as $(\frac{df}{dR} - 1)|_{z=0}$. For convenience, f_{R0} is often expressed as a logarithmic function of $|f_{R0}|$, i.e., $\log_{10}|f_{R0}|$. When $\log_{10}|f_{R0}|$ is smaller, the strength of modified gravity is weaker. The relationship between $\log_{10}|f_{R0}|$ and b is dependent on the specific model employed. For the three models utilized in this study, $\log_{10}|f_{R0}|$ is a function of b , Λ and R . The closer b is to 0, the smaller $\log_{10}|f_{R0}|$ is, when fixing Λ and R .

2.3. Hubble Parameter in $f(R)$ Theory

Our investigation focuses on the cosmic late-time accelerating expansion phenomenon in the framework of the $f(R)$ theory, so it is necessary to obtain the corresponding Hubble parameters at different redshifts in this theory. It is noted that Equation (3) represents a fourth-order ODE with respect to the Hubble parameter. In principle, we can obtain the solution for the Hubble parameter at a given redshift by solving the ODE. However, this method yields a highly complex solution, giving rise to various issues during the computational process, such as

difficulties in integration using standard methods. To avoid these issues, Basilakos et al. (2013) introduced a perturbation method that involves expanding the Hubble parameter in $f(R)$ theory around the vicinity of the Hubble parameter in the Λ CDM model. To facilitate the use of the perturbation method described above, Equation (3) can be reformulated as follows

$$-f_R H^2(z) + \Omega_{m0}(1+z)^3 + \Omega_{r0}(1+z)^4 + \frac{f_R R - f}{6} = f_{RR} H^2(z) R'(z). \quad (20)$$

Subsequently, we perform a perturbative expansion of $E(z) = H(z)/H_0$ for the Hu–Sawicki model, Starobinsky model, and ArcTanh model around $b = 0$, as listed below respectively. Then we have

$$E_{\text{HS}}^2(z) = \frac{H_{\text{HS}}^2(z)}{H_0^2} = E_{\Lambda}^2(z) + b\delta E_{1,\text{HS}}^2(z) + b^2\delta E_{2,\text{HS}}^2(z) + \mathcal{O}(2), \quad (21)$$

$$E_{\text{St}}^2(z) = \frac{H_{\text{St}}^2(z)}{H_0^2} = E_{\Lambda}^2(z) + b^2\delta E_{1,\text{St}}^2(z) + b^4\delta E_{2,\text{St}}^2(z) + \mathcal{O}(2), \quad (22)$$

$$E_{\text{AcT}}^2(z) = \frac{H_{\text{AcT}}^2(z)}{H_0^2} = E_{\Lambda}^2(z) + b\delta E_{1,\text{AcT}}^2(z) + b^2\delta E_{2,\text{AcT}}^2(z) + \mathcal{O}(2), \quad (23)$$

where $E_{\Lambda}(z)$ is the standardized Hubble parameters in the Λ CDM model, which is given by

$$E_{\Lambda}^2(z) = \frac{H_{\Lambda}^2(z)}{H_0^2} = \Omega_{m0}(1+z)^3 + \Omega_{r0}(1+z)^4 + (1 - \Omega_{m0} - \Omega_{r0}). \quad (24)$$

Balancing computational precision and efficiency, perturbations are typically considered up to the second order (Basilakos et al. 2013). Since we mainly study the history of expansion during the matter-dominated period, for simplicity, we approximate $\Omega_{r0} = 0$ in our analysis. The specific forms of Equations (21), (22) and (23) have been obtained in Sultana et al. (2022) and shown in Appendix A.

3. Mock Data

3.1. Type Ia Supernovae

SNe Ia, serving as cosmic standard candles, are crucial in establishing the standard cosmological model. The measurement of the distance modulus of an SN Ia can effectively determine the luminosity distance d_L at a given redshift, limit the slope of the late-time expansion rate, and consequently constrain the cosmological parameters. The CSST-UDF survey is expected to cover a sky area of 9 square degrees with $250 \text{ s} \times 60$ exposures in two years, reaching a survey depth of

approximately $i = 26$ AB mag for 5σ point source detection in one exposure.

Wang et al. (2024) utilized the SALT3 (Kenworthy et al. 2021) model and associated supernova spectral energy distribution (SED) templates to generate mock light curves of SNe Ia and different types of core-collapse supernovae (CCSNe) for the CSST-UDF survey. Using the fitting results of mock SN Ia light curves, the SN Ia distance modulus at a given redshift can be derived by

$$\mu_B = m_B - M_B + \alpha x_1 - \beta c, \quad (25)$$

where m_B and M_B are the B band apparent and absolute magnitudes respectively, and x_1 and c are the light-curve parameters related to time-dependent variation and color. We can obtain the photometric redshift z , m_B , x_1 and c from the light-curve fitting process, and M_B , α and β are the nuisance parameters and set to be free parameters when fitting the cosmological parameters.

Following Wang et al. (2024), we generate the SN Ia mock data for the CSST-UDF survey based on the cosmological parameters from Planck 2018 to constrain the $f(R)$ theory, which contains about 1897 SNe Ia in the redshift range from $z = 0$ to 1.2. The fiducial values of the nuisance parameters are set to be $\alpha = 0.16$, $\beta = 3.0$, and $M_B = -19.25$. In Figure 1, we show the Hubble diagram as a function of the input redshift for the SN Ia mock data. We find that, as expected, the CSST-UDF survey can obtain a large fraction of high- z SNe Ia, which are about 80% and 15% of the total SN Ia sample at $z > 0.5$ and $z > 1$, respectively. Note that we do not consider the contamination of CCSNe in the fitting process of the cosmological parameters for simplicity, since it can be effectively suppressed in the data analysis and will not affect the results (Wang et al. 2024).

3.2. Baryon Acoustic Oscillation

We also make use of the BAO data given by Miao et al. (2023) to constrain the models of the $f(R)$ theory. The BAO mock data sets are derived from the CSST galaxy and active galactic nucleus (AGN) spectroscopic surveys, which cover the redshift ranges $z \in (0, 1.2)$ for galaxy survey and $z \in (0, 4)$ for the AGN survey. To reduce the nonlinear effect, the reconstruction technique is applied in the BAO analysis for the CSST galaxy survey. In Figure 2, we plot the BAO data used in our work. The data for the Hubble distance D_H/r_d and comoving angular diameter distance D_M/r_d are shown in the left and right panels, respectively, where r_d is the size of the sound horizon at the drag epoch. The BAO data are divided into four redshift bins for both CSST galaxy and AGN surveys, and we set the systematic error of the calibration of the slitless spectroscopic survey $N_{\text{sys}} = 0$ and $10^4 h^{-3} \text{ Mpc}^3$ as the optimistic and pessimistic cases, respectively. The BAO mock data are derived based on the Λ CDM model, using the

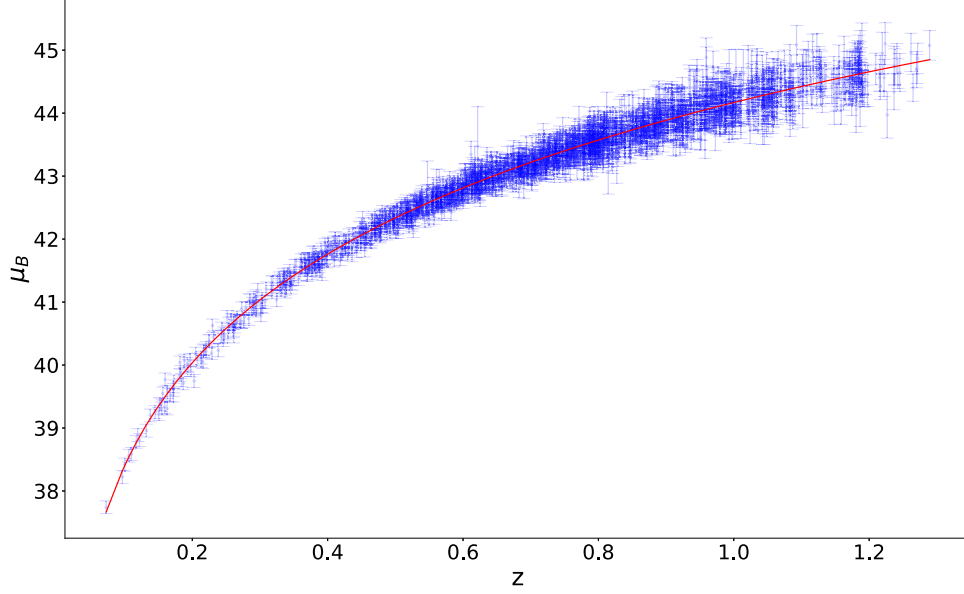


Figure 1. The mock data of distance modulus as a function of the input redshift for the SN Ia survey in the CSST-UDF. The red solid curve represents the theoretical distance modulus using the fiducial values of the cosmological parameters and nuisance parameters in the SN Ia model.

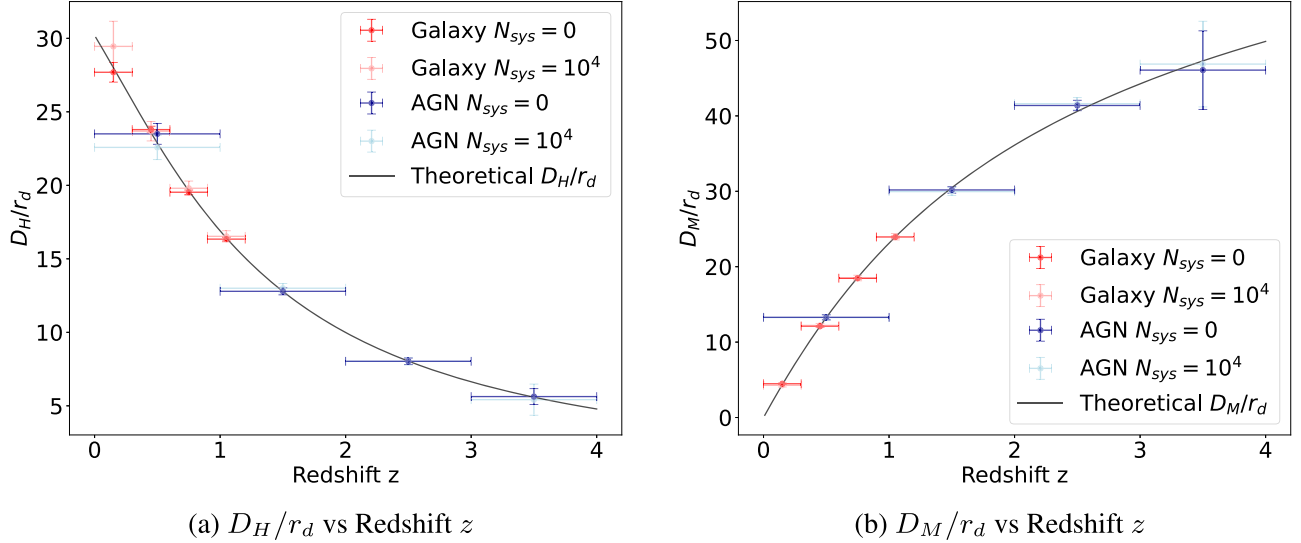


Figure 2. The BAO mock data of the CSST slitless spectroscopic galaxy (red) and AGN (blue) surveys from Miao et al. (2023). The data of D_H/r_d and D_M/r_d are shown in the left and right panels, respectively. We also consider the systematic error $N_{\text{sys}} = 0$ and $10^4 h^{-3} \text{ Mpc}^3$ as the optimistic and pessimistic cases respectively. The solid black curves signify the theoretical curves assuming the fiducial cosmological parameters.

cosmological parameters derived from the Planck 2018 results as the fiducial values, which is the same as the SN Ia case.

4. Model Fitting and Comparison

We adopt Markov Chain Monte Carlo (MCMC) methods to constrain the cosmological parameters of the $f(R)$ models. The likelihood function can be estimated as $\mathcal{L} \propto \exp(-\frac{\chi^2}{2})$, where

χ^2 is the chi-square. For an SN Ia, it can be expressed as

$$\chi_{\text{SN}}^2 = \sum_i \frac{(\mu_{\text{obs}}^i - \mu_{\text{th}})^2}{\sigma_{\text{SN},i}^2}, \quad (26)$$

where μ_{obs} and μ_{th} are the observational and theoretical distance moduli respectively, and σ_{SN} is the data error. Since an SN Ia is produced by the explosion of a white dwarf accreting

material greater than the Chandrasekhar limit, its absolute magnitude M_B is related to the gravitational constant G . In the $f(R)$ model, G is no longer a constant, but can vary as a function of time or redshift, i.e., $G_{f(R)}(z)$, which can be written as (Kumar et al. 2023)

$$G_{f(R)}(z) = \frac{G}{f_R} \left(\frac{1 + 4k^2 m/a^2}{1 + 3k^2 m/a^2} \right), \quad (27)$$

where $m = \frac{f_{RR}}{f_R}$ and $k = 0.1 h \text{ Mpc}^{-1}$. Then the theoretical SN Ia distance modulus will be corrected as (Gaztañaga et al. 2001; Wright & Li 2018)

$$\mu_{f(R)} = 5 \log_{10} \left(\frac{d_L}{\text{Mpc}} \right) + 25 + \frac{15}{4} \log_{10} \left(\frac{G_{f(R)}(z)}{G} \right). \quad (28)$$

Here $d_L(z)$ is the luminosity distance for an object at redshift z , and it can be expressed by

$$d_L(z) = c(1+z) \int_0^z \frac{1}{H(z')} dz'. \quad (29)$$

The chi-square of BAO for both galaxy and AGN surveys is given by

$$\chi_{\text{BAO}}^2 = \chi_{\parallel}^2 + \chi_{\perp}^2 = \sum_i \frac{[(D_H/r_d)_{\text{obs}}^i - (D_H/r_d)_{\text{th}}]^2}{\sigma_{\parallel,i}^2} + \sum_i \frac{[(D_M/r_d)_{\text{obs}}^i - (D_M/r_d)_{\text{th}}]^2}{\sigma_{\perp,i}^2}. \quad (30)$$

Theoretically, the feature of BAO along the line of sight can be characterized by the Hubble distance $D_H(z) = c/H(z)$, and that perpendicular to the line of sight can be described by the comoving angular diameter distance

$$D_M(z) = c \int_0^z \frac{dz'}{H(z')}. \quad (31)$$

In theory, r_d is related to the speed of sound $c_s(z)$ (Brieden et al. 2023), which is given by

$$r_d = \int_{\infty}^{z_d} \frac{c_s(z)}{H(z)} dz = \frac{147.05}{\text{Mpc}} \left(\frac{\Omega_m h^2}{0.1432} \right)^{-0.23} \times \left(\frac{N_{\text{eff}}}{3.04} \right)^{-0.1} \left(\frac{\Omega_b h^2}{0.02235} \right)^{-0.13}. \quad (32)$$

Here we fix the effective number of neutrino species $N_{\text{eff}} = 3.04$ and the baryon density $\Omega_b = 0.02235 \pm 0.00037$ (Schöneberg et al. 2019, 2022) in the fitting process.

Then we can obtain the joint likelihood function, and it takes the form

$$\mathcal{L}_{\text{tot}}(D_{\text{tot}}|\theta_1, \theta_2) = \mathcal{L}_{\text{SN}}(D_{\text{SN}}|\theta_1) \times \mathcal{L}_{\text{BAO}}(D_{\text{BAO}}|\theta_2) \propto \exp \left[-\frac{1}{2} (\chi_{\text{SN}}^2 + \chi_{\text{BAO}}^2) \right], \quad (33)$$

where D denotes the data set, $\theta_1 = (\alpha, \beta, M_B, h, \Omega_{m0}, b)$ and $\theta_2 = (h, \Omega_{m0}, b)$. We employ `emcee`⁶ to perform the MCMC process (Foreman-Mackey et al. 2013), subsequently constraining the cosmological parameters of the three $f(R)$ models using the CSST SN Ia, BAO, and SN Ia+BAO mock data, respectively. We assume flat priors for the free parameters in the model, and we have $\alpha \in [0.11, 0.17]$, $\beta \in [2.55, 3.15]$, $M_B \in [-19.35, -19.15]$, $h \in [0.65, 0.75]$, $\Omega_{m0} \in [0.0, 0.6]$, and $b \in [-1.0, 1.0]$. We employ 30 walkers to randomly explore the parameter space for 100,000 steps. The first 100 steps are rejected as the burn-in process. After thinning the chains, we obtain about 30,000 chain points to illustrate the probability distribution functions (PDFs) of the model parameters in each case.

We also utilize the Akaike Information Criterion (AIC), Bayesian Information Criterion (BIC), χ_{reduced}^2 and natural logarithm of the Bayesian evidence ($\ln \mathcal{Z}$) to compare the $f(R)$ models to the Λ CDM model. Here $\text{AIC} = -2 \ln \mathcal{L}(\theta_{\text{fit}}) + 2k$, $\text{BIC} = -2 \ln \mathcal{L}(\theta_{\text{fit}}) + k \ln n$, $\chi_{\text{reduced}}^2 = \chi_{\text{min}}^2 / n_{\text{dof}}$ and $\mathcal{Z} = \int \mathcal{L}(D|\theta, M) P(\theta|M) d\theta$, where θ_{fit} is the best-fitting value, k is the number of parameters, n is the number of data points, $n_{\text{dof}} = n - k$ is the degrees of freedom, χ_{min}^2 is the minimum chi-square, and $P(\theta|M)$ is the prior distribution of the parameter θ given a model M .

5. Result and Discussion

In Figure 3, we show the predicted 2D contour maps and 1D PDFs of the parameters in the three $f(R)$ models for the CSST SN Ia and BAO surveys. The details of the constraint results are listed in Table 1. Based on our utilization of observational data derived from the cosmological simulations with $b = 0$, we anticipate that the constraint on b should be around 0, and similarly for (h, Ω_{m0}) centered around (0.673, 0.313). As we can see, Figure 3 shows that all parameter constraint results are positioned closely around their fiducial values, which matches well with the expectation.

As can be seen in Figure 3 and Table 1, the constraints on Ω_{m0} and h in the Λ CDM model are more stringent than those in the $f(R)$ models, since there is an additional parameter b in the $f(R)$ models. The constraint results from the CSST BAO survey are basically better than the CSST-UDF SN Ia survey for these two parameters, even considering $N_{\text{sys}} = 10^4 h^{-3} \text{ Mpc}^3$ in the BAO data. Note that the current constraint accuracy on h can reach $\sim 3\%$ in the CSST-UDF SN Ia survey, and this is because we have assumed a relatively narrow prior range for M_B , which has strong degeneracy with h . We can find that the joint constraints on Ω_{m0} and h in the $f(R)$ models can achieve 1%–2% and 3%–8% accuracy for the CSST SN Ia+BAO mock data.

⁶ <https://github.com/dfm/emcee>

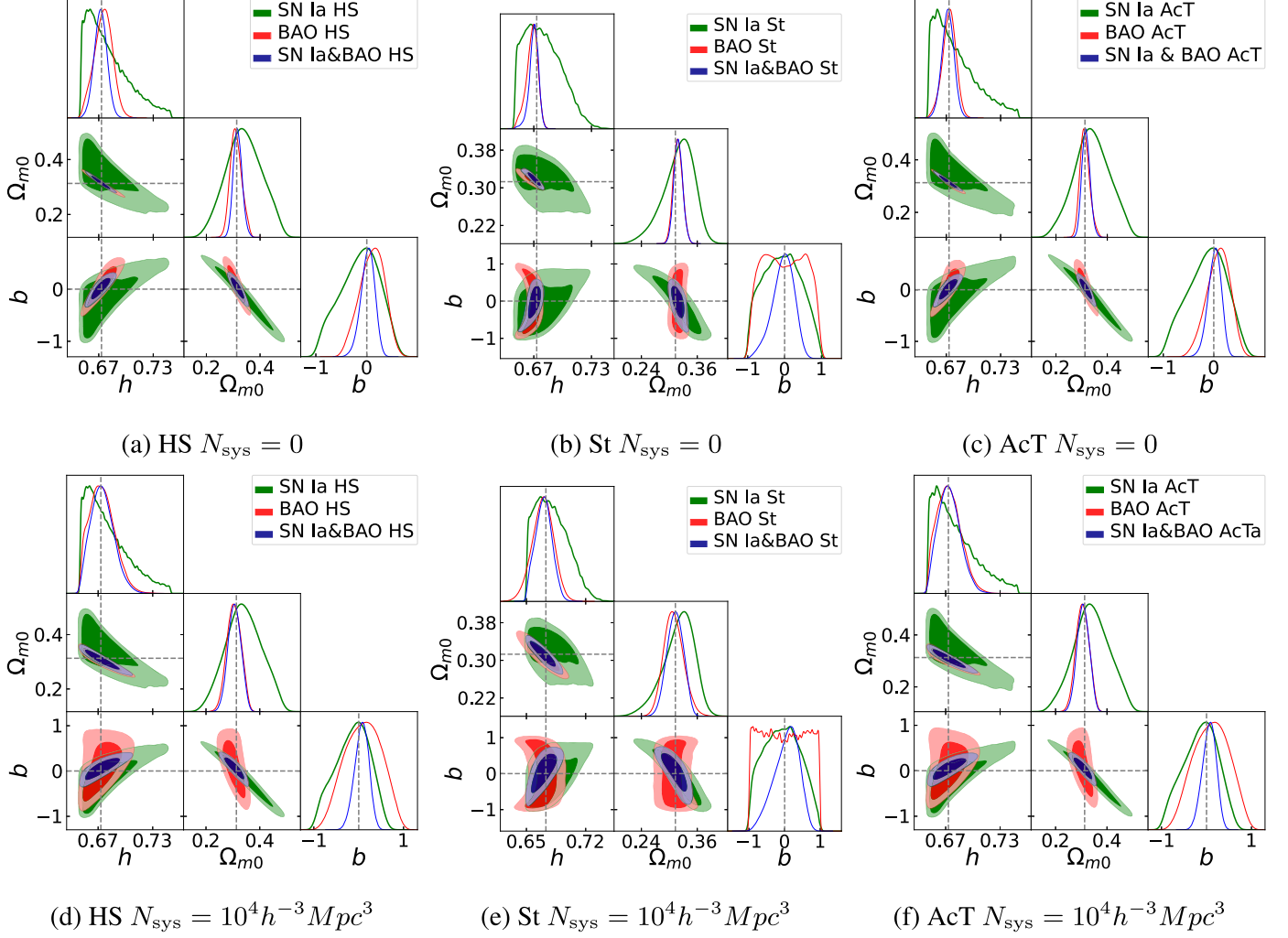


Figure 3. The 1σ and 2σ contour maps and 1D PDFs of the parameters in the three $f(R)$ models for the CSST SN Ia and BAO mock data. We study the constraint results by assuming $N_{\text{sys}} = 0$ (upper panels) and $10^4 h^{-3} \text{Mpc}^3$ (lower panels) for the BAO data. The dashed lines represent the fiducial parameter values.

For the $f(R)$ model parameter b , the constraint results are similar for the Hu–Sawicki model and the ArcTanh model, and can restrict b within about ± 0.4 and ± 0.3 for the CSST SN Ia and BAO surveys, respectively. The joint constraint can improve the result to be within ± 0.2 using the CSST SN Ia+BAO mock data. However, the constraints on b become much worse for the Starobinsky model, which give the results within about ± 0.6 , ± 0.7 , and ± 0.5 for the SN Ia, BAO, and SN Ia+BAO data, respectively. This implies that the parameter b in the Starobinsky model is not as sensitive as the other models to the SN Ia and BAO data, which is also indicated by other studies, e.g., Sultana et al. (2022); Kumar et al. (2023). In addition, we also explore the constraint accuracy of $\log_{10}|f_{R0}|$ corresponding to the three models based on the MCMC chains. We find that the accuracies can reach 21%, 33%, and 19% for the Hu–Sawicki, Starobinsky

and ArcTanh models, respectively. Comparing our constraints to the results using the current observational data, e.g., Kumar et al. (2023), we find that, the precision of parameter constraints on the $f(R)$ models by the CSST SN Ia+BAO data set is comparable to or even higher than that of the eBOSS-BAO (Alam et al. 2021) + BBN (Aver et al. 2015) + PantheonPlus&SH0ES (Brout et al. 2022) data set.

We also perform model comparison with the ΛCDM model by calculating ΔAIC , ΔBIC , $\Delta\chi^2_{\text{reduced}}$, and $\Delta\ln\mathcal{Z}$, and the results are displayed in Table 2. As expected, all of the criteria of model comparison distinctly prefer the ΛCDM model to the $f(R)$ model, since we have assumed it as our fiducial model in the mock data generation and analysis. This indicates that the CSST SN Ia and BAO data are accurate enough to put strong constraints on the $f(R)$ theory and can distinguish it from the

Table 1
The Best-Fits and 1σ Errors of the Parameters in the Λ CDM and Three $f(R)$ Models Constrained by the CSST SN Ia and BAO Mock Data

Dateset	Model	h	Ω_{m0}	b
SN Ia	Λ CDM	$0.685^{+0.014}_{-0.025}$ (2.88%)	$0.317^{+0.016}_{-0.010}$ (4.15%)	...
	Hu–Sawicki	$0.661^{+0.044}_{-0.003}$ (3.52%)	$0.330^{+0.081}_{-0.057}$ (20.83%)	$0.086^{+0.169}_{-0.643}$
	Starobinsky	$0.666^{+0.034}_{-0.006}$ (3.00%)	$0.330^{+0.022}_{-0.044}$ (9.96%)	$0.010^{+0.466}_{-0.628}$
	ArcTanh	$0.659^{+0.045}_{-0.002}$ (3.55%)	$0.334^{+0.078}_{-0.063}$ (21.00%)	$0.026^{+0.232}_{-0.578}$
BAO($N_{\text{sys}} = 0$)	Λ CDM	0.672 ± 0.004 (0.62%)	$0.317^{+0.010}_{-0.008}$ (2.86%)	...
	Hu–Sawicki	$0.677^{+0.008}_{-0.012}$ (1.49%)	$0.304^{+0.029}_{-0.013}$ (7.09%)	$0.153^{+0.195}_{-0.301}$
	Starobinsky	$0.671^{+0.003}_{-0.009}$ (0.88%)	0.318 ± 0.010 (3.10%)	$0.001^{+0.618}_{-0.616}$
	ArcTanh	$0.675^{+0.005}_{-0.009}$ (1.10%)	$0.308^{+0.024}_{-0.014}$ (6.07%)	$0.211^{+0.112}_{-0.359}$
BAO($N_{\text{sys}} = 10^4$)	Λ CDM	$0.674^{+0.012}_{-0.009}$ (1.56%)	$0.298^{+0.027}_{-0.011}$ (6.32%)	...
	Hu–Sawicki	$0.669^{+0.019}_{-0.009}$ (2.10%)	$0.300^{+0.031}_{-0.023}$ (8.92%)	$0.253^{+0.279}_{-0.585}$
	Starobinsky	$0.670^{+0.012}_{-0.013}$ (1.87%)	$0.302^{+0.028}_{-0.014}$ (6.90%)	-0.005 ± 0.688
	ArcTanh	$0.675^{+0.012}_{-0.015}$ (1.99%)	$0.304^{+0.027}_{-0.024}$ (8.45%)	$0.111^{+0.418}_{-0.424}$
SN Ia + BAO($N_{\text{sys}} = 0$)	Λ CDM	$0.671^{+0.004}_{-0.003}$ (0.54%)	$0.317^{+0.010}_{-0.006}$ (2.39%)	...
	Hu–Sawicki	0.672 ± 0.007 (1.07%)	$0.316^{+0.017}_{-0.015}$ (5.12%)	$0.037^{+0.116}_{-0.153}$
	Starobinsky	$0.671^{+0.004}_{-0.005}$ (0.68%)	$0.318^{+0.010}_{-0.008}$ (2.93%)	$0.024^{+0.229}_{-0.360}$
	ArcTanh	$0.672^{+0.006}_{-0.007}$ (0.98%)	$0.315^{+0.018}_{-0.014}$ (5.04%)	$0.027^{+0.121}_{-0.141}$
SN Ia + BAO($N_{\text{sys}} = 10^4$)	Λ CDM	$0.670^{+0.006}_{-0.007}$ (1.03%)	$0.312^{+0.015}_{-0.007}$ (3.51%)	...
	Hu–Sawicki	$0.672^{+0.015}_{-0.010}$ (1.89%)	$0.307^{+0.024}_{-0.024}$ (7.90%)	$0.089^{+0.133}_{-0.181}$
	Starobinsky	$0.671^{+0.009}_{-0.011}$ (1.48%)	$0.312^{+0.018}_{-0.018}$ (5.75%)	$0.152^{+0.246}_{-0.468}$
	ArcTanh	$0.675^{+0.011}_{-0.014}$ (1.81%)	$0.303^{+0.028}_{-0.019}$ (7.84%)	$0.092^{+0.121}_{-0.187}$

Table 2

Comparison Results of the Hu–Sawicki, Starobinsky, and ArcTanh Models with the Λ CDM Model Using the Four Model Comparison Methods of AIC, BIC, χ^2_{reduced} and $\ln \mathcal{Z}$ for Each Dataset

Dataset	Model	ΔAIC	ΔBIC	$\Delta\chi^2_{\text{reduced}}$	$\Delta \ln \mathcal{Z}$
SN Ia	HS	1.6577	7.2057	0.0002	-0.0551
	St	1.7768	7.3248	0.0003	-0.0805
	AcT	1.6447	7.1927	0.0002	-0.0749
BAO $N_{\text{sys}} = 0$	HS	1.7623	1.8418	0.1917	-0.1539
	St	1.8623	1.9417	0.2117	-0.0279
	AcT	1.7706	1.8500	0.1933	-0.1761
BAO $N_{\text{sys}} = 10^4$	HS	1.9841	2.0635	0.1335	-0.1527
	St	1.9477	2.0271	0.1262	0.0241
	AcT	1.9844	2.0638	0.1336	-0.1493
SN Ia + BAO $N_{\text{sys}} = 0$	HS	1.9422	7.4944	0.0004	-0.2139
	St	2.1088	7.6610	0.0004	-0.2297
	AcT	1.9599	7.5122	0.0004	-0.2165
SN Ia + BAO $N_{\text{sys}} = 10^4$	HS	1.8254	7.3776	0.0003	-0.1426
	St	1.7610	7.3132	0.0003	-0.1308
	AcT	1.8062	7.3585	0.0003	-0.1468

Λ CDM model at a high significance level. We also show the constraint results of the nuisance parameters in the CSST-UDF SN Ia survey, i.e., α , β and M_B in Appendix B.

6. Summary and Conclusion

In this work, we employ the simulated CSST SN Ia and BAO data to study the constraint power on the relevant parameters of the three $f(R)$ theoretical models, i.e., the Hu–Sawicki, Starobinsky and ArcTanh models. The high-precision simulated observational data of the CSST can provide us with a good validation channel for the future constraint ability of the CSST on the $f(R)$ modified gravity theory. First, following the steps outlined by Basilakos et al. (2013) and Sultana et al. (2022), we obtained the expansion rate $H(z)$ for the three models. Then we use the CSST SN Ia and BAO mock data provided by Wang et al. (2024) and Miao et al. (2023) to constrain the three $f(R)$ theories. We find that the CSST SN Ia and BAO surveys can provide stringent constraints on the $f(R)$ models. Compared to the current results using similar kinds of observational data, the constraints on the $f(R)$ models by the CSST SN Ia+BAO joint data set are comparable or even higher. Besides, if considering other CSST surveys, e.g., weak gravitational lensing and galaxy clustering surveys, the constraint result can be further significantly improved. Therefore, we can expect that, by performing a joint analysis of these CSST cosmological probes, CSST is able to constrain and distinguish the $f(R)$ theory and the Λ CDM theory with a high-precision.

Acknowledgments

J.H.Y. and Y.G. acknowledge the support from the National Key R&D Program of China grant Nos. 2022YFF0503404, 2020SKA0110402, and the CAS Project for Young Scientists in Basic Research (No. YSBR092). X.C. acknowledges the support of the National Natural Science Foundation of China (NSFC, grant Nos. 11473044 and 11973047), and the Chinese Academy of Science grants ZDKYYQ20200008, QYZDJ-SSW-SLH017, XDB 23040100, and XDA15020200. This work is also supported by science research grants from the

China Manned Space Project with grant Nos. CMS-CSST-2021-B01 and CMS-CSST-2021-A01.

Appendix A $E(z)$ in the Three $f(R)$ Models

The expressions for $E(z)$ in the Hu–Sawicki, Starobinsky and ArcTanh $f(R)$ models we use are shown below for reference.
Hu–Sawicki model:

$$\begin{aligned}
 E_{\text{HS}}^2(z) = & \frac{H_{\text{HS}}(z)^2}{H_0^2} = 1 - \Omega_{m0} + (1+z)^3 \Omega_{m0} \\
 & + \frac{6b(-1 + \Omega_{m0})^2(4(-1 + \Omega_{m0})^2 + (1+z)^3(-1 + \Omega_{m0})\Omega_{m0} - 2(1+z)^6\Omega_{m0}^2)}{(1+z)^9 \left(\frac{4(-1 + \Omega_{m0})}{(1+z)^3} - \Omega_{m0} \right)^3} \\
 & + \frac{b^2(-1 + \Omega_{m0})^3}{(1+z)^{24} \left(-\frac{4(-1 + \Omega_{m0})}{(1+z)^3} + \Omega_{m0} \right)^8} (1024(-1 + \Omega_{m0})^6 \\
 & + 9216(1+z)^3(-1 + \Omega_{m0})^5\Omega_{m0} - 22848(1+z)^6(-1 + \Omega_{m0})^4\Omega_{m0}^2 \\
 & + 25408(1+z)^9(-1 + \Omega_{m0})^3\Omega_{m0}^3 - 7452(1+z)^{12}(-1 + \Omega_{m0})^2\Omega_{m0}^4 \\
 & - 4656(1+z)^{15}(-1 + \Omega_{m0})\Omega_{m0}^5 \\
 & + 37(1+z)^{18}\Omega_{m0}^6)
 \end{aligned} \tag{A1}$$

Starobinsky model:

$$\begin{aligned}
 E_{\text{St}}^2(z) = & \frac{H_{\text{St}}(z)^2}{H_0^2} = 1 - \Omega_{m0} + (1+z)^3 \Omega_{m0} \\
 & + \frac{b^2(-1 + \Omega_{m0})^3(32(-1 + \Omega_{m0})^2 + 32(1+z)^3(-1 + \Omega_{m0})\Omega_{m0} - 37(1+z)^6\Omega_{m0}^2)}{(1+z)^{12} \left(-\frac{4(-1 + \Omega_{m0})}{(1+z)^3} + \Omega_{m0} \right)^4} \\
 & + \frac{b^4(-1 + \Omega_{m0})^5}{(1+z)^{30} \left(-\frac{4(-1 + \Omega_{m0})}{(1+z)^3} + \Omega_{m0} \right)^{10}} \times (20480(-1 + \Omega_{m0})^6 + 63488(1+z)^3(-1 + \Omega_{m0})^5\Omega_{m0} \\
 & - 234880(1+z)^6(-1 + \Omega_{m0})^4\Omega_{m0}^2 + 289024(1+z)^9(-1 + \Omega_{m0})^3\Omega_{m0}^3 \\
 & - 44552(1+z)^{12}(-1 + \Omega_{m0})^2\Omega_{m0}^4 - 82748(1+z)^{15}(-1 + \Omega_{m0})\Omega_{m0}^5 \\
 & + 123(1+z)^{18}\Omega_{m0}^6).
 \end{aligned} \tag{A2}$$

ArcTanh model:

$$\begin{aligned}
E_{\text{AcT}}^2(z) = & \frac{H_{\text{AcT}}(z)^2}{H_0^2} = 1 - \Omega_{m0} + (1+z)^3 \Omega_{m0} \\
& + \frac{2b(-1 + \Omega_{m0})^2}{3(1+z)^{15} \left(\frac{4(-1 + \Omega_{m0})}{(1+z)^3} - \Omega_{m0} \right)^5} (596(-1 + \Omega_{m0})^4 \\
& - 109(1+z)^3(-1 + \Omega_{m0})^3 \Omega_{m0} - 361(1+z)^6(-1 + \Omega_{m0})^2 \Omega_{m0}^2 \\
& + 153(1+z)^9(-1 + \Omega_{m0}) \Omega_{m0}^3 - 18(1+z)^{12} \Omega_{m0}^4) + \frac{b^2(-1 + \Omega_{m0})^3}{9(1+z)^{36} \left(-\frac{4(-1 + \Omega_{m0})}{(1+z)^3} + \Omega_{m0} \right)^{12}} \\
& \times (4189184(-1 + \Omega_{m0})^{10} + 23851008(1+z)^3(-1 + \Omega_{m0})^9 \Omega_{m0} - 95032704(1+z)^6(-1 + \Omega_{m0})^8 \Omega_{m0}^2 \\
& + 149808704(1+z)^9(-1 + \Omega_{m0})^7 \Omega_{m0}^3 - 110911572(1+z)^{12}(-1 + \Omega_{m0})^6 \Omega_{m0}^4 \\
& + 28668900(1+z)^{15}(-1 + \Omega_{m0})^5 \Omega_{m0}^5 + 2987537(1+z)^{18}(-1 + \Omega_{m0})^4 \Omega_{m0}^6 \\
& - 3144240(1+z)^{21}(-1 + \Omega_{m0})^3 \Omega_{m0}^7 + 636102(1+z)^{24}(-1 + \Omega_{m0})^2 \Omega_{m0}^8 \\
& - 47232(1+z)^{27}(-1 + \Omega_{m0}) \Omega_{m0}^9 + 333(1+z)^{30} \Omega_{m0}^{10})
\end{aligned} \tag{A3}$$

Appendix B

Constraints on the Nuisance Parameters in the SN Ia Model

In Figure B1, we show the posterior distribution of the SN Ia-related nuisance parameters under the Hu–Sawicki, Starobinsky, and ArcTanh $f(R)$ models after the MCMC process for a given prior. The details of the constraint results are shown in Table B1.

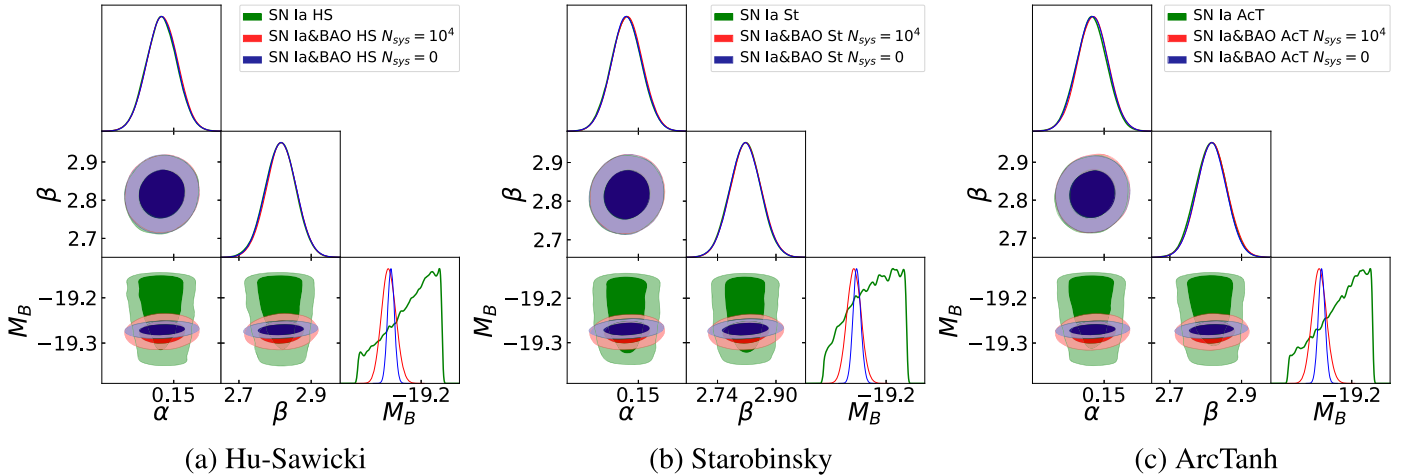


Figure B1. The contour maps and PDFs of the nuisance parameters α , β and M_B in the SN Ia model for the three $f(R)$ models, constrained by the CSST SN Ia and SN Ia+BAO mock data with $N_{\text{sys}} = 0$ and $10^4 h^{-3} \text{ Mpc}^3$.

Table B1

The Constraint Results of the SN Ia-Related Nuisance Parameters in Λ CDM, Hu–Sawicki, Starobinsky, and ArcTanh Models Restricted by the SN Ia and SN Ia +BAO Mock Data with $N_{\text{sys}} = 0$ and $10^4 h^{-3} \text{ Mpc}^3$

Model	Dateset	α	β	M_B
Λ CDM	SN Ia	$0.147^{+0.004}_{-0.003}$	$2.818^{+0.040}_{-0.044}$	$-19.213^{+0.034}_{-0.092}$
	SN Ia+BAO($N_{\text{sys}} = 0$)	$0.147^{+0.004}_{-0.003}$	$2.812^{+0.047}_{-0.037}$	$-19.155^{+0.016}_{-0.133}$
	SN Ia+BAO($N_{\text{sys}} = 10^4$)	$0.147^{+0.003}_{-0.004}$	$2.816^{+0.044}_{-0.039}$	$-19.281^{+0.019}_{-0.014}$
HS	SN Ia	$0.147^{+0.004}_{-0.003}$	$2.816^{+0.041}_{-0.043}$	$-19.155^{+0.016}_{-0.133}$
	SN Ia+BAO($N_{\text{sys}} = 0$)	$0.148^{+0.003}_{-0.004}$	$2.818^{+0.041}_{-0.044}$	$-19.270^{+0.008}_{-0.008}$
	SN Ia+BAO($N_{\text{sys}} = 10^4$)	$0.147^{+0.004}_{-0.003}$	$2.810^{+0.049}_{-0.034}$	$-19.276^{+0.017}_{-0.016}$
St	SN Ia	$0.147^{+0.003}_{-0.004}$	$2.817^{+0.041}_{-0.043}$	$-19.187^{+0.012}_{-0.107}$
	SN Ia+BAO($N_{\text{sys}} = 0$)	$0.147^{+0.004}_{-0.003}$	$2.806^{+0.053}_{-0.031}$	$-19.269^{+0.009}_{-0.010}$
	SN Ia+BAO($N_{\text{sys}} = 10^4$)	$0.148^{+0.003}_{-0.004}$	$2.822^{+0.038}_{-0.046}$	$-19.274^{+0.015}_{-0.018}$
AcT	SN Ia	$0.147^{+0.003}_{-0.004}$	$2.805^{+0.052}_{-0.033}$	$-19.173^{+0.002}_{-0.115}$
	SN Ia+BAO($N_{\text{sys}} = 0$)	$0.147^{+0.003}_{-0.004}$	$2.816^{+0.044}_{-0.039}$	$-19.281^{+0.019}_{-0.014}$
	SN Ia+BAO($N_{\text{sys}} = 10^4$)	$0.148^{+0.003}_{-0.004}$	$2.822^{+0.038}_{-0.046}$	$-19.273^{+0.014}_{-0.019}$

ORCID iDs

Xuele Chen  <https://orcid.org/0000-0001-6475-8863>

References

- Alam, S., Aubert, M., Avila, S., et al. 2021, *PhRvD*, **103**, 083533
- Aver, E., Olive, K. A., & Skillman, E. D. 2015, *JCAP*, **2015**, 011
- Basilakos, S., Nesseris, S., & Perivolaropoulos, L. 2013, *PhRvD*, **87**, 123529
- Bean, R., Bernat, D., Pogossian, L., Silvestri, A., & Trodden, M. 2007, *PhRvD*, **75**, 064020
- Brieden, S., Gil-Marín, H., & Verde, L. 2023, *JCAP*, **04**, 023
- Brout, D., Scolnic, D., Popovic, B., et al. 2022, *ApJ*, **938**, 110
- Capozziello, S., & Tsujikawa, S. 2008, *PhRvD*, **77**, 107501
- Casas, S., Cardone, V. F., Sapone, D., et al. 2023, arXiv:2306.11053
- Chiba, T., Smith, T. L., & Erickcek, A. L. 2007, *PhRvD*, **75**, 124014
- Dainotti, M. G., De Simone, B., Montani, G., & Bogdan, M. 2024, in Multifrequency Behaviour of High Energy Cosmic Sources XIV (Trieste: SISSA)
- De Felice, A., & Tsujikawa, S. 2010, *LRR*, **13**, 3
- Faraoni, V. 2006, *PhRvD*, **74**, 104017
- Foreman-Mackey, D., Hogg, D. W., Lang, D., & Goodman, J. 2013, *PASP*, **125**, 306
- Gaztañaga, E., García-Berro, E., Isern, J., Bravo, E., & Domínguez, I. 2001, *PhRvD*, **65**, 023506
- Hu, W., & Sawicki, I. 2007, *PhRvD*, **76**, 064004
- Kenworthy, W. D., Jones, D. O., Dai, M., et al. 2021, *ApJ*, **923**, 265
- Koyama, K. 2016, *PPh*, **79**, 046902
- Kumar, S., Nunes, R. C., Pan, S., & Yadav, P. 2023, *PDU*, **42**, 101281
- LSST Dark Energy Science Collaboration 2012, arXiv:1211.0310
- Liu, X., Li, B., Zhao, G., et al. 2016, *PhRvL*, **117**, 051101
- Miao, H., Gong, Y., Chen, X., et al. 2023, *MNRAS*, **532**, 3991
- Nojiri, S., Odintsov, S., & Oikonomou, V. 2017, *PhR*, **692**, 1
- Nojiri, S., & Odintsov, S. D. 2006, *PhLB*, **637**, 139
- Nojiri, S., & Odintsov, S. D. 2011, *PhR*, **505**, 59
- Pérez-Romero, J., & Nesseris, S. 2018, *PhRvD*, **97**, 023525
- Perlmutter, S., Aldering, G., Goldhaber, G., et al. 1999, *ApJ*, **517**, 565
- Planck Collaboration, Aghanim, N., Akrami, Y., et al. 2020, *A&A*, **641**, A6
- Qi, Y., Yang, W., Wang, Y., et al. 2023, *PDU*, **40**, 101180
- Riess, A. G., et al. 1998, *AJ*, **116**, 1009
- Saridakis, E., Lazkoz, R., Salzano, V., et al. 2021, arXiv:2105.12582
- Schöneberg, N., Lesgourgues, J., & Hooper, D. C. 2019, *JCAP*, **2019**, 029
- Schöneberg, N., Verde, L., Gil-Marín, H., & Brieden, S. 2022, *JCAP*, **2022**, 039
- Starobinsky, A. A. 1980, *PhLB*, **91**, 99
- Starobinsky, A. A. 2007, *JETPL*, **86**, 157
- Sultana, J., Yennapureddy, M. K., Melia, F., & Kazanas, D. 2022, *MNRAS*, **514**, 5827
- Wang, M., Gong, Y., Deng, F., et al. 2024, *MNRAS*, **530**, 4288
- Wright, B. S., & Li, B. 2018, *PhRvD*, **97**, 083505